

# Mott-Kondo Insulator Behavior in the Iron Oxychalcogenides

B. Freelon,<sup>1,2\*</sup> Yu Hao Liu,<sup>1</sup> Jeng-Lung Chen,<sup>1,3</sup> L. Craco,<sup>4\*</sup> M. S. Laad,<sup>5</sup> S. Leoni,<sup>6</sup> Jiaqi Chen,<sup>7</sup> Li Tao,<sup>7</sup> Hangdong Wang,<sup>7</sup> R. Flauca,<sup>8</sup> Z. Yamani,<sup>8</sup> Minghu Fang,<sup>7</sup> Chinglin Chang,<sup>3</sup> J.-H. Guo<sup>1</sup> and Z. Hussain<sup>1\*</sup>

<sup>1</sup> *Advanced Light Source Division, Lawrence Berkeley National Laboratory, One Cyclotron Road, Berkeley, CA 94720*

<sup>2</sup> *Advanced Photon Source, Argonne National Laboratory, Argonne, Illinois 60439*

<sup>3</sup> *Department of Physics, Tamkang University, Tamsui, Taiwan 250*

<sup>4</sup> *Instituto de Física, Universidade Federal de Mato Grosso, 78060-900, Cuiabá, MT, Brazil*

<sup>5</sup> *The Institute of Mathematical Sciences, C.I.T. Campus, Chennai 600 113, India*

<sup>6</sup> *School of Chemistry, Cardiff University, Cardiff, CF10 3AT, UK*

<sup>7</sup> *Department of Physics, Zhejiang University, Hangzhou 310027, P. R. China*

<sup>8</sup> *Canadian Neutron Beam Centre, National Research Council, Chalk River Laboratories, Chalk River, Ontario K0J 1J0, Canada*

(Dated: October 19, 2018)

We perform a combined experimental-theoretical study of the Fe-oxychalcogenides (FeO*Ch*) series  $\text{La}_2\text{O}_2\text{Fe}_2\text{OM}_2$  ( $M=\text{S, Se}$ ), which is the latest among the Fe-based materials with the potential to show unconventional high- $T_c$  superconductivity (HTSC). A combination of incoherent Hubbard features in X-ray absorption (XAS) and resonant inelastic X-ray scattering (RIXS) spectra, as well as resistivity data, reveal that the parent FeO*Ch* are correlation-driven insulators. To uncover microscopics underlying these findings, we perform local density approximation-plus-dynamical mean field theory (LDA+DMFT) calculations that unravel a Mott-Kondo insulating state. Based upon good agreement between theory and a range of data, we propose that FeO*Ch* may constitute a new, ideal testing ground to explore HTSC arising from a strange metal proximate to a novel selective-Mott quantum criticality.

PACS numbers: 74.70.Xa, 74.70.-b, 74.25.F-, 74.25.Jb

Since the discovery [1] of high-temperature superconductivity (HTSC) in iron pnictides (FePn), a fundamental question has been whether the iron pnictides are weakly correlated metals or bad metals in close proximity to Mott localization [2, 3]. These competing ideas must imply very different mechanisms of Fe-based HTSC. The Mottness view proposes that strong, orbitally-selective electron correlation is relevant to HTSC, while the competing itinerant view holds that antiferromagnetic (AFM) order and superconductivity (SC) originate from a Kohn-Luttinger-like Fermi surface (FS) nesting mechanism with weak electronic correlations [4]. Early insights suggested the importance of varying the strength [2, 5] of electron correlations using chemical substitutions to tune systems across band-width driven Mott localization. Since then, more evidence has accumulated in support of this proposal; FeSe is a bad-metal without AF order [6], while parent Fe-oxychalcogenides are electrical insulators [7, 8].

Most FePn superconductors exhibit bad-metal normal states with hints of novel quantum criticality. The discovery of HTSC in alkaline iron selenides  $A_{1-x}\text{Fe}_{2-y}\text{Se}_2$ , where  $A = \text{K, Tl, Cs}$  and  $\text{Rb}$  (referred to as "245s") intensified this basic debate, since SC with  $T_c = 30$  K emerges from doping an AFM insulating state occurring due to Fe-vacancy induced band narrowing [9]. Studying more such materials to further develop a complete description of the generic electronic phase diagram of iron superconductors is clearly warranted. With this in mind, we investigated iron oxychalcogenides such as  $X_2\text{OFe}_2\text{O}_2M_2$  [ $X=(\text{La, Na, Ba})$ , ( $M=(\text{S, Se})$ ] [10] because of (i) their similarities to LaFeOAs (1111) materials and (ii) the opportunity to study materials with slightly larger electron correlation than the pnictides [7]. Moreover,  $\text{La}_2\text{O}_2\text{Fe}_2\text{OM}_2$  ( $M=\text{S, Se}$ ) offer the attractive option to tune the strength of electronic correlations in one system through disorder-free chalcogen replacement of S by Se. The FeO*Ch* consist of stacked double-layered units  $\text{La}_2\text{O}_2$  and  $\text{Fe}_2\text{O}(\text{S, Se})_2$ .  $\text{Fe}_2\text{O}(\text{S, Se})_2$  contains an Fe layer that is similar to the FeAs layer in the pnictides; in the latter,  $\text{Fe}^{2+}$  ( $d^6$  configuration) is co-ordinated by O atoms but there is an extra Oxygen atom O(2). The rare-earth layer also contains an additional O(1) atom. Chalcogen substitution results in a slightly expanded Fe-square-lattice unit cell of  $\text{La}_2\text{O}_2\text{Fe}_2\text{OM}_2$  compared to that of LaOFeAs [10]. The consequent decrease in the electronic bandwidth  $W$  must increase the Hubbard  $U$ , offering a disorder-free parameter to subtly tune  $U/W$  across a critical value for a Mott insulator phase.

Na, Ba), ( $M=(\text{S, Se})$ ] [10] because of (i) their similarities to LaFeOAs (1111) materials and (ii) the opportunity to study materials with slightly larger electron correlation than the pnictides [7]. Moreover,  $\text{La}_2\text{O}_2\text{Fe}_2\text{OM}_2$  ( $M=\text{S, Se}$ ) offer the attractive option to tune the strength of electronic correlations in one system through disorder-free chalcogen replacement of S by Se. The FeO*Ch* consist of stacked double-layered units  $\text{La}_2\text{O}_2$  and  $\text{Fe}_2\text{O}(\text{S, Se})_2$ .  $\text{Fe}_2\text{O}(\text{S, Se})_2$  contains an Fe layer that is similar to the FeAs layer in the pnictides; in the latter,  $\text{Fe}^{2+}$  ( $d^6$  configuration) is co-ordinated by O atoms but there is an extra Oxygen atom O(2). The rare-earth layer also contains an additional O(1) atom. Chalcogen substitution results in a slightly expanded Fe-square-lattice unit cell of  $\text{La}_2\text{O}_2\text{Fe}_2\text{OM}_2$  compared to that of LaOFeAs [10]. The consequent decrease in the electronic bandwidth  $W$  must increase the Hubbard  $U$ , offering a disorder-free parameter to subtly tune  $U/W$  across a critical value for a Mott insulator phase.

In this Letter, we substantiate this reasoning by presenting first measurements of the unoccupied and occupied Fe and Oxygen density-of-states (DOS) obtained by soft X-ray absorption (XAS) and resonant inelastic X-ray scattering (RIXS). Strong Fe moment localization that can be tuned with chalcogen replacement, and, more crucially, the observation of incoherent Fe spectral weight due to Hubbard band formation marks the FeO*Ch* as correlation-driven insulators. The incoherent spectral weight undergoes a resonant enhancement in the RIXS data and LHB spectral weight analysis, indicat-

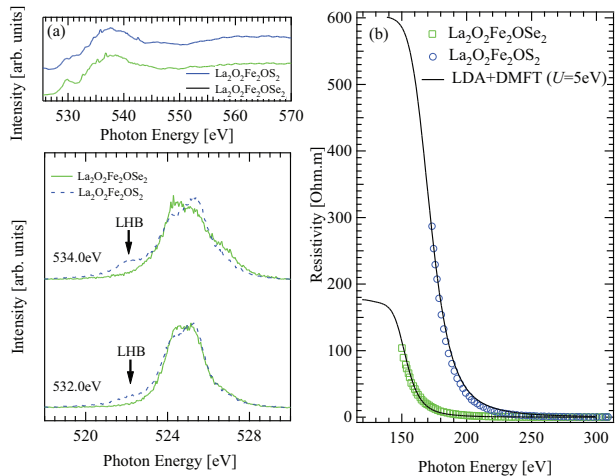


FIG. 1: (Color online) (a) O  $1s$  XAS and (b) O  $K\alpha$  RIXS data for  $\text{La}_2\text{O}_2\text{Fe}_2\text{OM}_2$ , ( $M = \text{S}, \text{Se}$ ). RIXS intensity data was collected using photons with incident energies of 532 and 534 eV. In (c) the electrical resistivity versus temperature  $T$  data and the simulated resistivity calculated using LDA + DMFT is shown.

ing the Mott insulating character of both  $\text{La}_2\text{O}_2\text{Fe}_2\text{OS}_2$  and  $\text{La}_2\text{O}_2\text{Fe}_2\text{OSe}_2$ . We discuss the implications of these findings for possible HTSC arising from an incoherent metal proximate to novel selective-Mott quantum criticality.

We investigated well characterized  $\text{La}_2\text{O}_2\text{Fe}_2\text{OM}_2$  ( $M=\text{S}, \text{Se}$ ) polycrystalline materials, with nominal compositions, that were fabricated using solid state reactions methods described earlier [7]. High purity  $\text{La}_2\text{O}_3$ , Fe and (S, Se) powders were used as starting materials and laboratory X-ray powder diffraction data showed that these materials had minimal impurity phases; neutron powder diffraction data confirmed this finding.

XAS and RIXS spectra for the  $\text{FeOCh}$  were collected in a polarization averaged condition. In order to reduce the possibility of oxidation, iron oxychalcogenide samples were sheared under a pressure of  $10^{-6}$  Torr in a pre-chamber immediately before being placed in the ultra-high vacuum experimental chamber. All present measurements were performed in the paramagnetic state above 150 K. The Advanced Light Source beamlines 7.0.1 and 8.0.1 delivered X-ray beams of 100 micron spot-sizes and energy resolutions of 0.2 eV (0.2 eV) and 0.5 eV (0.6 eV) for oxygen(iron) X-ray absorption and emission, respectively. The oxygen  $K$ -edge XAS intensity is proportional to the unoccupied  $p$ -weighted DOS resulting from the  $\Delta l = \pm 1$  dipole selection rule for X-ray photon absorption. If the Fe-O related bond is partially covalent, O  $2p$  states hybridize with Fe  $3d$  orbitals and hence the pre-threshold for absorption, i.e., the low energy fine structure, reveals itself in ligand-to-metal charge transfer excitations [11]. XAS is sensitive to metal

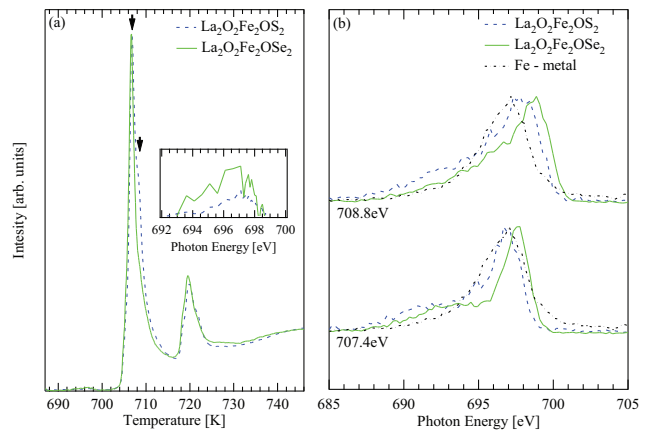


FIG. 2: (Color online) The Fe  $L_{2,3}$ -edge XAS profiles of  $\text{La}_2\text{O}_2\text{Fe}_2\text{OM}_2$ , ( $M = \text{S}, \text{Se}$ ) is shown in panel (a). The arrows indicate the X-ray absorption features at the photon energies, 707.4 and 708.8 eV, used to collect the Fe RIXS data in (b). The data are plotted with a vertical offset for clarity.

atom coordination geometry and  $3d$  occupation (oxidation state). Fig. 1, top panel (a), shows the O  $K$  XAS profiles of  $\text{La}_2\text{O}_2\text{Fe}_2\text{OM}_2$  ( $M = \text{S}, \text{Se}$ ). Incident X-ray energies of 532 and 534 eV were used to collect the O  $K\alpha$  RIXS data presented in Fig. 1 (a). The presence of lower Hubbard band (LHB) structure in  $\text{La}_2\text{O}_2\text{Fe}_2\text{OS}_2$  RIXS spectra is consistent with resistivity data (Fig. 1 (b)) which shows  $M = \text{S}$  to be a better insulator than  $M = \text{Se}$ . We note the absence of O charge transfer band, i.e., a high energy shoulder structure for the O  $2p$  mainband peak, in the Oxygen RIXS data of  $\text{La}_2\text{O}_2\text{Fe}_2\text{OSe}_2$  material: this suggests that the extent of Fe-O hybridization DOS is different for  $M = \text{S}$  and  $M=\text{Se}$  compounds.

In Fig. 2 (a), we show the Fe  $L_{2,3}$ -edge XAS spectra for both  $\text{La}_2\text{O}_2\text{Fe}_2\text{OS}_2$  and  $\text{La}_2\text{O}_2\text{Fe}_2\text{OSe}_2$ . A magnification (inset) of the region near the Fermi level, presented in Fig. 2 (a), reveal a clear difference in the iron conduction band weight of the two materials.  $\text{La}_2\text{O}_2\text{Fe}_2\text{OSe}_2$  has enhanced spectral weight at pre-edge just above  $E_F$ , and this must ultimately be related to details of the *correlated* electronic structure changes upon replacement of S by Se. Fe XAS data is consistent with both RIXS and bulk measurements that show  $M = \text{Se}$  to be less strongly correlated than  $M = \text{S}$ . Resonant inelastic X-ray scattering (RIXS) intensity data, see Fig. 2 (b), were collected using incident X-ray energies tuned to near- and off-resonance Fe X-ray absorption features at 707.4 eV and 708.8 eV, respectively. RIXS [12] intensity results from a second-order (i.e., two-step) photon-in, photon-out process that can be described by the Kramers-Heisenberg (KH) relationship [12]. The KH expression requires the enhancement of the scattering intensity when incident photon energy matches X-ray absorption edge energies. The RIXS data for  $M = \text{S}$  shows correlation induced broad features in the high energy spectral re-

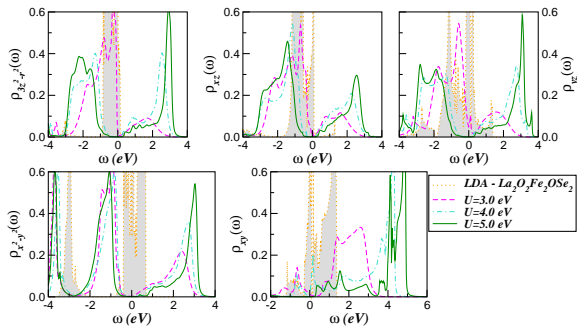


FIG. 3: (Color online) Orbital-resolved LDA density-of-states (DOS) for the Fe  $d$  orbitals of  $\text{La}_2\text{O}_2\text{Fe}_2\text{OSe}_2$  as well as LDA+DMFT results for different values of  $U$  (with  $U' = U - 2J_H$ ) and fixed  $J_H = 0.7$  eV. Notice the narrow bands in the LDA DOS. Compared to the LDA results, large spectral weight transfer along with electronic localization is visible in the LDA+DMFT spectral functions for  $U \geq 4$  eV.

gion that form the LHB. In the RIXS data, for both  $M = \text{S, Se}$ , there is a high intensity Fe  $3d$  metal valence band peak. Near 692 eV, a broad shoulder in the high energy spectral region is resonantly enhanced. The spectra clearly reveal incoherent electronic excitations involving  $3d$  Fe electrons. These are correlation satellites formed by multi-particle excitations that involve localized states, and clearly reveal the stronger electronic correlations that generate a correlated insulator in the  $\text{FeOCh}$ .

Taken together, these results mark the  $\text{FeOCh}$  as correlated, bandwidth-control driven insulators [13]. In multi-orbital  $\text{FeOCh}$  with strong inter-orbital charge transfer, correlations and crystal field effects, proper characterization of the Mott insulating state(s) is an important, non-trivial issue. To shed light on microscopics underlying the above findings, we performed LDA+DMFT calculations for the  $\text{FeOCh}$  closely following earlier work [8, 14]. LDA calculations were performed within the linear muffin-tin orbitals (LMTO) scheme. The one-electron Hamiltonian reads  $H_0 = \sum_{k,a,\sigma} \epsilon_a(k) c_{k,a,\sigma}^\dagger c_{k,a,\sigma}$  with  $a = xy, xz, yz, x^2 - y^2, 3z^2 - r^2$  label (diagonalized in orbital basis) five Fe  $3d$  bands. We retain only the  $d$  states, since the non- $d$  orbital DOS have negligible or no weight at  $E_F$ . An important aspect of our study is readily visible in Fig. 3 which shows a sizable reduction of the LDA bandwidth relative to that of  $\text{FeSe}$  (which is itself an incoherent bad-metal [15]), induced by hybridization with  $O$  states and distorting effects of the La-layers. Another interesting aspect, in contrast to Fe-arsenides, is that the  $xz - yz$  orbital degeneracy in the tetragonal structure is explicitly removed at the outset. Thus, in  $\text{FeOCh}$ , an electronic nematic (EN) instability linked to ferro-orbital order and its potentially related critical-

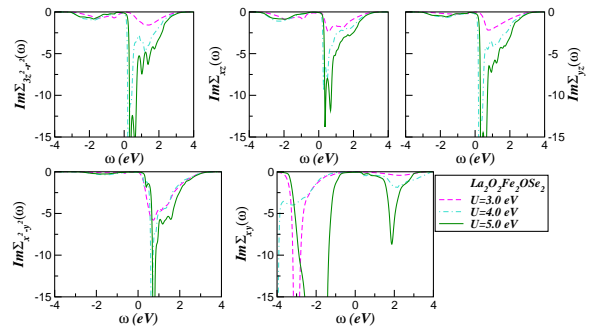


FIG. 4: (Color online) Orbital-resolved imaginary parts of the DMFT self-energies for the Fe  $d$  orbitals of  $\text{La}_2\text{O}_2\text{Fe}_2\text{OSe}_2$  for different values of  $U$  and  $J_H = 0.7$  eV.

ity is not relevant. Finally, clear lower-dimensional band structural features are visible in  $\rho_{LDA}^{xz}(\omega)$  (quasi-1D) and  $\rho_{LDA}^{xy}(\omega)$  (2D van-Hove singular) near the Fermi energy,  $E_F (= 0)$ . Enhancement of the *effective*  $U/W$  ratio in such an intrinsically anisotropic setting should now naturally favor the Mott insulator state in  $\text{FeOCh}$ . To substantiate this, DMFT calculations were performed using the multi-orbital iterated perturbation theory (MO-IPT) as an impurity solver. Though not exact, MO-IPT has a proven record of providing reliable results for a number of correlated systems [16], and is a very efficient and fast solver for arbitrary  $T$  and band-filling. The full Hamiltonian is  $H = H_0 + H_1$  with  $H_1 = U \sum_{i,a} n_{ia\downarrow} n_{ia\uparrow} + \sum_{i,a \neq b} [U' n_{ia} n_{ib} - J_H \mathbf{S}_{ia} \cdot \mathbf{S}_{ib}]$ , with  $U' = (U - 2J_H)$  being the inter-orbital Coulomb term and  $J_H$  the local Hund's coupling. Though  $U \simeq 4.0 - 5.0$  eV and  $J_H = 0.7$  eV are expected, we vary  $3.0 \leq U \leq 5.0$  to get more insight.

In Fig. 3, we show the total many-body local spectral function (DOS) for the  $M = \text{Se}$  case. A clear transition from a bad-metal state at  $U = 3.0$  eV to a correlated insulator for  $U = 4.0, 5.0$  eV occurs. Looking closely at the self-energies in Fig. 4, however, a remarkable aspect

stands out:  $\text{Im}\Sigma_a(\omega = E_F)$  vanishes in the region of the Mott gap, instead of having a pole, as would occur in a true Mott insulator. This aspect is more reminiscent of a correlated *Kondo* insulator, where the gap arises due to combined effects of electronic correlations and sizable interband hybridization. While this novel finding is somewhat unexpected, proximity to a true Mott state is seen by observing that the pole structures in  $\text{Im}\Sigma_a(\omega)$  with  $a = xz, yz, 3z^2 - r^2$  lie only slightly above  $E_F$ . Thus, because the system *is* correlated, sizable spectral redistribution in response to additional small perturbations (e.g. longer-range Coulomb interactions in an insulator) can drive it into a true Mott insulating phase. More importantly, electron doping will also generically cause

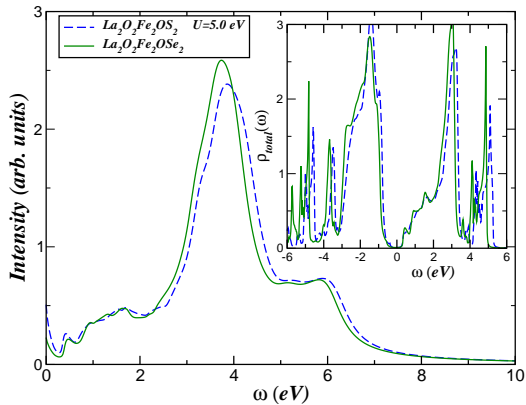


FIG. 5: (Color online) Total LDA+DMFT XAS spectrum of  $\text{La}_2\text{O}_2\text{Fe}_2\text{O}_2M_2$  ( $M = \text{S}, \text{Se}$ ), showing the changes in the upper Hubbard band upon chalcogen substitution. Inset shows the corresponding total LDA+DMFT spectral function for  $U = 5.0$  eV and  $J_H = 0.7$  eV.

large-scale orbital-selective (OS) spectral weight transfer, leading to orbital-selective Mott transition (OSMT), wherein a subset of orbital states remain (Mott) gapped in an incoherent metallic state [8]. Such states can exhibit novel quantum criticality associated with an endpoint of the OSMT. Whether HTSC near such novel criticality occurs in suitably doped  $\text{FeOCh}$  is an enticing and open issue.

Remarkably, a comparison to Fe-edge XAS and  $dc$  resistivity data reveals good agreement, providing support for this novel finding. In Fig. 5, we show our LDA+DMFT XAS spectrum. We have incorporated the relevant effects of core-hole scattering for XAS line-shapes by consistently adapting the procedure of Pardini *et al.* [17] within our DMFT scheme. Several important aspects stand out: (i) there is good semi-quantitative accord with the Fe-edge XAS data up to 3.0 eV above  $E_F$ . More importantly, details of the differences in spectral weight between  $M = \text{S}$  and  $M = \text{Se}$  cases is also in very good accord with data, (ii) enhanced spectral weight at pre-edge just above  $E_F$ , just as seen, while smearing of lower energy structures ( $0.0 < \omega < 2.0$  eV) and higher energy of the 3.0 eV peak for  $M = \text{S}$  relative to  $M = \text{Se}$  is in good accord, both with XAS data, as well as with resistivity data which show  $M = \text{S}$  to be more correlated than  $M = \text{Se}$ . Indeed, LDA+DMFT resistivities (using the Kubo formalism and neglecting vertex corrections to the conductivity, which are negligible [18]) for  $M = \text{S}, \text{Se}$  show very good accord with experiment (where  $\rho_{dc}^{(M)}(T)$  was measured above 150 K. This is a strong internal self-consistency check, and puts our novel proposal on stronger ground.

Armed with these positive features, we now discuss

their implications for possible HTSC in suitably doped or pressurized systems. Both are expected to tune the Fe-O hybridization: since we find a correlated Mott-Kondo insulator, this must non-trivially reconstruct the Fe- $d$  states. In  $\text{La}_2\text{O}_2\text{Fe}_2\text{OSe}_2$ , suppression of oxygen Hubbard-band spectral weight presages the onset of bad-metallicity even as the localization of the Fe  $3d$  states is preserved. This may provide clues to metallize  $\text{FeOCh}$  by appropriately manipulating the Oxygen and chalcogen states which hybridize with Fe- $d$  states. This is an exciting perspective because, if HTSC results, (as in 245s), it would reinforce the fundamental challenge to the itinerancy perspective in pnictide HTSC research. Specifically, since strong correlations have now obliterated the LDA FS as above, large-scale orbital-selective redistribution of spectral weight upon carrier doping is generically expected to lead to OSMT and FS involving only a subset of original  $d$ -orbitals. The LDA FS and its nesting features can now no longer serve as a guide for rationalizing instabilities to novel order(s). Instead, strong electronic scattering between the partially (Mott) localized and itinerant subsets of the many-body spectral functions generically extinguishes the Landau quasiparticle (QP) pole at  $E_F$ . In absence of a QP description for the normal state, the very tenability of the FS nesting scenario is called into doubt.

Thus, our work provides an impetus to consider closer similarities between Fe-based systems and the cuprates.

In similarity with 245 materials, we suggest that  $\text{FeOCh}$  are ideal candidates for testing this proposal. The development of incoherent scattering observed in our XAS and RIXS spectra arises from Mott localized states. If these can be appropriately doped, it is likely that strong orbitally-selective scattering will nearly extinguish the Landau-Fermi liquid quasiparticles, leading to the emergence of an incoherent pseudogapped metal reminiscent of underdoped cuprates [8]. Whether novel quantum criticality associated with a selective-Mott transition in conjunction with the development of HTSC in  $\text{FeOCh}$  will be seen in the future is of great interest. Our findings provide a compelling motivation to produce and study doped or pressurized iron oxychalcogenides.

After the recent journal submission of this paper, we learned of work by G. Giovannetti *et al.* on the iron oxychalcogenides which is complementary to ours and gives comparable results.

The Advanced Light Source is supported by the Director, Office of Science, Office of Basic Energy Sciences, of the U.S. Department of Energy (DOE), under Contract No. DE-AC02-05CH11231. ZJU work is supported by the National Basic Research Program of China (973 Program) under Grants No. 2011CBA00103 and 2012CB821404, the National Science Foundation of China (No. 11374261, 11204059) and Zhejiang Provincial Natural Science Foundation of China (No. LQ12A04007). M.S.L thanks MPIPES, Dresden for hos-

pitality. L.C.'s work was supported by CAPES - Proc. No. 002/2012. Acknowledgment (L.C.) is also made to FAPEMAT/CNPq (Project: 685524/2010) and the Physical Chemistry department at Technical University Dresden for hospitality.

---

\* Electronic address: [freelon@mit.edu](mailto:freelon@mit.edu),  
[lcraco@fisica.ufmt.br](mailto:lcraco@fisica.ufmt.br)

- [1] Y. Kamihara, T. Watanabe, M. Hirano, and H. Hosono, *J. Am. Chem. Soc.* **130**, 3296 (2008).
- [2] Si, Qimiao and Abrahams, Elihu, *Phys. Rev. Lett.* **101**, 076401 (2008).
- [3] M. R. Norman, *Physics* **1**, 21 (2008).
- [4] A. V. Chubukov, D. V. Efremov, and I. Eremin, *Phys. Rev. B* **78**, 134512 (2008).
- [5] G. Baskaran, *J. Phys. Soc. Jap.* **77**, 113713 (2008).
- [6] T. Imai, K. Ahilan, F. L. Ning, T. M. McQueen, and R. J. Cava, *Phys. Rev. Lett.* **102**, 177005 (2009).
- [7] J.-X. Zhu, R. Yu, H. Wang, L. L. Zhao, M. D. Jones, J. Dai, E. Abrahams, E. Morosan, M. Fang, and Q. Si, *Phys. Rev. Lett.* **104**, 216405 (2010).
- [8] L. Craco, M. S. Laad, and S. Leoni, *J. Phys.: Condensed Matter* **26**, 145602 (2014).
- [9] M.-H. Fang, H.-D. Wang, C.-H. Dong, Z.-J. Li, C.-M. Feng, J. Chen, and H. Q. Yuan, *Europhys. Lett.* **94**, 27009 (2011).
- [10] J. M. Mayer, L. F. Schneemeyer, T. Siegrist, J. V. Waszczak, and B. Van Dover, *Angewandte Chemie International Edition in English* **31**, 1645 (1992).
- [11] F. M. F. de Groot, M. Grioni, J. C. Fuggle, J. Ghijsen, G. A. Sawatzky, and H. Petersen, *Phys. Rev. B* **40**, 5715 (1989).
- [12] A. Kotani and S. Shin, *Rev. Mod. Phys.* **73**, 203 (2001).
- [13] M. Imada, A. Fujimori, and Y. Tokura, *Rev. Mod. Phys.* **70**, 1039 (1998).
- [14] L. Craco, M. S. Laad, and S. Leoni, *Phys. Rev. B* **84**, 224520 (2011).
- [15] L. Craco, M. S. Laad, and S. Leoni, *Europhys. Lett.* **91**, 27001 (2010).
- [16] A. Georges, G. Kotliar, W. Krauth, and M. J. Rozenberg, *Rev. Mod. Phys.* **68**, 13 (1996).
- [17] L. Pardini, V. Bellini, and F. Manghi, *J. of Phys.: Condensed Matter* **23**, 215601 (2011).
- [18] J. M. Tomczak and S. Biermann, *J. Phys.: Condensed Matter* **21**, 064209 (2009).